2

Conceptual foundations

學而不思則罔，思而不學則殆
If one studies but does not think, one will be bewildered. If one thinks but does not study, one will be in peril.

(Confucius)

2.1 Introduction

This chapter presents the conceptual foundations of plasma turbulence theory from the perspective of physical kinetics of quasi-particles. It is divided into two sections:

(1) Dressed test particle model of fluctuations in a plasma near equilibrium;
(2) K41 beyond dimensional analysis – revisiting the theory of hydrodynamic turbulence.

The reason for this admittedly schizophrenic beginning is the rather unusual and atypical niche that plasma turbulence occupies in the pantheon of turbulent and chaotic systems. In many ways, most (though not all) cases of plasma turbulence may be thought of as weak turbulence, spatiotemporal chaos or wave turbulence, as opposed to fully developed turbulence in neutral fluids. Dynamic range is large, but nonlinearity is usually *not* overwhelmingly strong. Frequently, several aspects of the linear dynamics persist in the turbulent state, though wave breaking is possible, too. While a scale-to-scale transfer is significant, local emission and absorption, at a particular scale, are not negligible. Scale invariance is usually only approximate, even in the absence of dissipation. Indeed, it is fair to say that plasma turbulence lacks the elements of simplicity, clarity and universality which have attracted many researchers to the study of high Reynolds number fluid turbulence. In contrast to that famous example, plasma turbulence is a problem in the dynamics of a *multi-scale and complex system*. It challenges the researcher to isolate, define and solve interesting and relevant thematic or idealized problems which illuminate the more complex and intractable whole. To this end, then, it is useful to begin by discussing two rather different 'limiting case paradigms', which in some sense

'bound' the position of most plasma turbulence problems in the intellectual realm. These limiting cases are:

- The test particle model (TPM) of a near-equilibrium plasma, for which the relevant quasi-particle is a dressed test particle;
- The Kolmogorov (K41) model of a high Reynolds number fluid, very far from equilibrium, for which the relevant quasi-particle is the fluid eddy.

The TPM illustrates important plasma concepts such as local emission and absorption, screening response and the interaction of waves and sources (Balescu, 1963; Ichimaru, 1973). The K41 model illustrates important turbulence theory concepts such as scale similarity, cascades, strong energy transfer between scales and turbulent dispersion (Kolmogorov, 1941). We also briefly discuss turbulence in two dimensions – very relevant to strongly magnetized plasmas – and turbulence in pipe flows. The example of turbulent pipe flow, usually neglected by physicists in deference to homogeneous turbulence in a periodic box, is especially relevant to plasma confinement, as it constitutes *the* prototypical example of eddy viscosity and mixing length theory, and of profile formation by turbulent transport. The prominent place that engineering texts accord to this deceptively simple example is no accident – engineers, after all, need answers to real world problems. More fundamentally, just as the Kolmogorov theory is a basic example of self-similarity in scale, the Prandtl mixing length theory nicely illustrates self-similarity in space (Prandtl, 1932). The choice of these two particular paradigmatic examples is motivated by the huge disparity in the roles of spectral transfer and energy flux in their respective dynamics. In the TPM, spectral transport is ignorable, so the excitation at each scale k is determined by the local balance of excitation and damping at that scale. In the inertial range of turbulence, local excitation and damping are negligible, and all scales are driven by spectral energy flux – i.e. the cascade – set by the dissipation rate. (See Figure 2.1 for illustration.) These two extremes correspond, respectively, to a state with no flux and to a flux-driven state, in some sense 'bracket' most realizations of (laboratory) plasma turbulence, where excitation, damping and transfer are all roughly comparable. For this reason, they stand

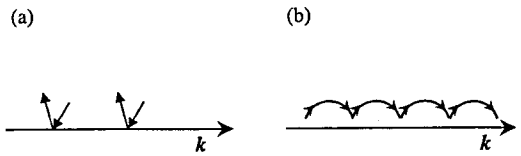

Fig. 2.1. (a) Local in k emission and absorption near equilibrium. (b) Spectral transport from emission at k_1, to absorption at k_2 via nonlinear coupling in a non-equilibrium plasma.

out as conceptual foundations, and so we begin out study of plasma turbulence with them.

2.2 Dressed test particle model of fluctuations in a plasma near equilibrium

2.2.1 Basic ideas

Virtually *all* theories of plasma kinetics and plasma turbulence are concerned, in varying degrees, with calculating the fluctuation spectrum and relaxation rate for plasmas under diverse circumstances. The simplest, most successful and best known theory of plasma kinetics is the *dressed test particle model* of fluctuations and relaxation in a plasma near equilibrium. This model, as presented here, is a synthesis of the pioneering contributions and insights of Rostoker and Rosenbluth (1960), Balescu (1963), Lenard (1960), Klimontovich (1967), Dupree (1961), and others. The unique and attractive feature of the test particle model is that it offers us a physically motivated and appealing picture of dynamics near equilibrium which is *entirely consistent* with Kubo's linear response theory and the fluctuation–dissipation theorem (Kubo, 1957; Callen and Welton, 1951), but does *not* rely upon the abstract symmetry arguments and operator properties that are employed in the more formal presentations of generalized fluctuation theory, as discussed in texts such as Landau and Lifshitz' *Statisical Physics* (1980). Thus, *the test particle model is consistent with formal fluctuation theory, but affords the user far greater physical insight.* Though its applicability is limited to the rather simple and seemingly dull case of a stable plasma 'near' thermal equilibrium, the test particle model nevertheless constitutes a vital piece of the conceptual foundation upon which all the more exotic kinetic theories are built. For this reason we accord it a prominent place in our study, and begin our journey by discussing it in some depth.

Two questions of definition appear immediately at the outset. These are:

(a) What is a plasma?
(b) What does 'near equilibrium' mean?

For our purposes, a plasma is a quasi-neutral gas of charged particles with thermal energy far in excess of electrostatic energy (i.e. $k_B T \gg q^2/\bar{r}$), and with many particles within a Debye sphere (i.e. $1/n\lambda_D^3 \ll 1$), where q is a charge, $\bar{r}$ is a mean distance between particles, $\bar{r} \sim n^{-1/3}$, n is a mean density, T is a temperature, and k_B is the Boltzmann constant. The first property distinguishes a gaseous plasma from a liquid or crystal, while the second allows its description by a Boltzmann equation. Specifically, the condition $1/n\lambda_D^3 \ll 1$ means that discrete particle effects are, in some sense, 'small' and so allows truncation of the BBGKY (Bogoliubov, Born, Green, Kirkwood, Yvon) hierarchy at the level of a Boltzmann equation.

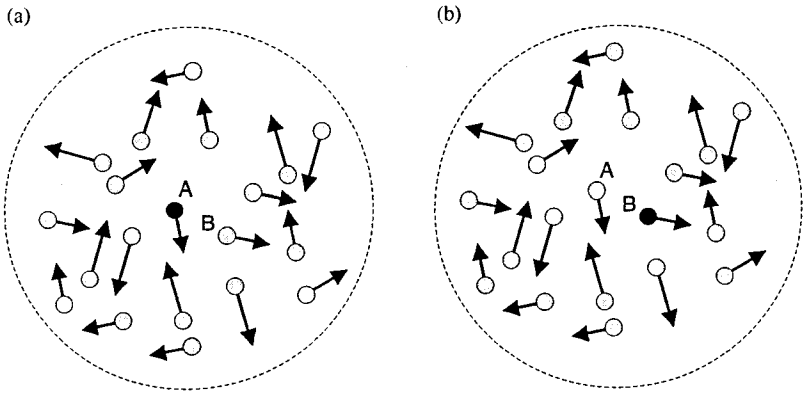

Fig. 2.2. A large number of particles exist within a Debye sphere of particle A (shown in black) in (a). Other particles provide a screening on the particle A. When the particle B is chosen as a test particle, others (including A) produce screening on B, (b). Each particle acts the role of test particle and the role of screening for the other test particle.

This is equivalent to stating that if the two body correlation $f(1,2)$ is written in a cluster expansion as $f(1)f(2)+g(1,2)$, then $g(1,2)$ is of $O(1/n\lambda_D^3)$ with respect to $f(1)f(2)$, and that higher order correlations are negligible. Figure 2.2 illustrates a test particle surrounded by many particle in a Debye sphere. The screening on the particle A is induced by other particles. When the particle B is chosen as a test particle, others (including A) produce screening of B. Each particle acts in the dual roles of a test particle and as part of the screening for other test particles.

The definition of 'near-equilibrium' is more subtle. A near-equilibrium plasma is one characterized by:

(1) a balance of emission and absorption by particles at a rate related to the temperature, T;
(2) the viability of linear response theory and the use of linearized particle trajectories.

Condition (1) necessarily implies the absence of linear instability of collective modes, but *does not* preclude collectively enhanced relaxation to states of higher entropy. Thus, a near-equilibrium state need not be one of maximum entropy. Condition (2) *does* preclude zero frequency convective cells driven by thermal fluctuations via mode–mode coupling, such as those that occur in the case of transport in 2D hydrodynamics. Such low frequency cells are usually associated with long time tails and require a renormalized theory of the nonlinear response for their description, as is discussed in later chapters.

The essential element of the test particle model is the compelling physical picture it affords us of the balance of emission and absorption which is intrinsic to

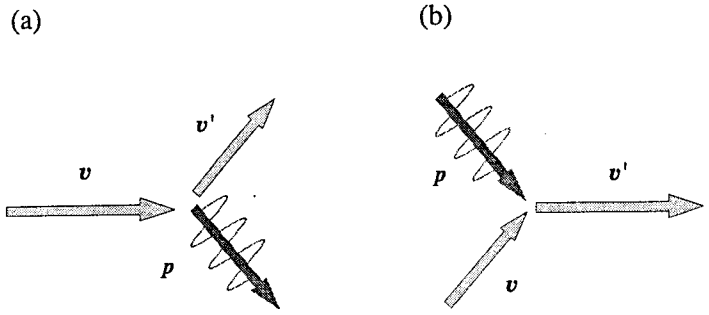

Fig. 2.3. Schematic drawing of the emission of the wave by one particle and the absorption of the wave.

thermal equilibrium. In the test particle model (TPM), *emission* occurs as a discrete particle (i.e. electron or ion) moves through the plasma, Cerenkov emitting electrostatic waves in the process. This emission process creates *fluctuations* in the plasma and converts particle kinetic energy (i.e. thermal energy) to collective mode energy. Wave radiation also induces a *drag* or dynamical friction on the emitter, just as the emission of waves in the wake of a boat induces a wave drag force on the boat. Proximity to equilibrium implies that emission is, in turn, balanced by *absorption*. Absorption occurs via Landau damping of the emitted plasma waves, and constitutes a wave energy dissipation process which heats the resonant particles in the plasma. Note that this absorption process ultimately returns the energy which was radiated by the particles to the thermal bath. The physics of wave emission and absorption which defines the thermal equilibrium balance intrinsic to the TPM is shown in Figure 2.3.

A distinctive feature of the TPM is that in it, each plasma particle has a 'dual identity', both as an 'emitter' and an 'absorber'. As an emitter, each particle radiates plasma waves, which are moving along some specified, linear, unperturbed orbit. Note that each emitter is identifiable (i.e. as a discrete particle) while moving through the Vlasov fluid, which is composed of other particles. As an absorber, each particle helps to define an element of the Vlasov fluid responding to, and (Landau) damping the emission from, *other* discrete particles. In this role, particle discreteness is smoothed over. Thus, the basic picture of an equilibrium plasma is one of a soup or gas of *dressed test particles*. In this picture, each particle:

(i) stimulates a collective response from the other particles by its discreteness;
(ii) responds to or 'dresses' other discrete particles by forming part of the background Vlasov fluid.

Thus, if one views the plasma as a pea soup, then the TPM is built on the idea that 'each pea in the soup acts like soup for all the other peas'. The *dressed test particle* is the *fundamental quasi-particle* in the description of near-equilibrium

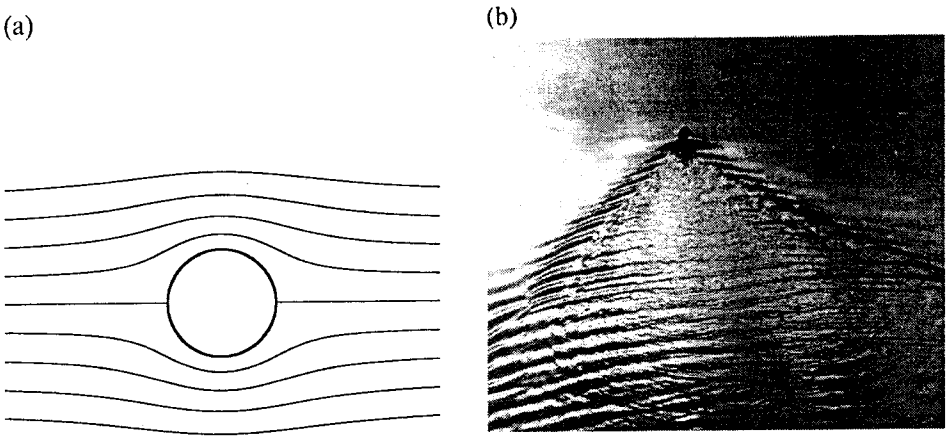

Fig. 2.4. Dressing of moving objects. Examples like a sphere in a fluid (a) and a supersonic object (b) are illustrated. In the case of a sphere, the surrounding fluid moves with it, so that the effective mass of the sphere (measured by the ratio between the acceleration to the external force) increases. The supersonic object radiates the wake of the sound wave.

plasmas. Examples for dressing by surrounding media are illustrated in Figure 2.4. In the case of a sphere in a fluid, the surrounding fluid moves with it, so that the effective mass of the sphere (defined by the ratio between the external force to the acceleration) increases by an amount $(2\pi/3)\,\rho a^3$, where a is the radius of the sphere and ρ is the mass density of the surrounding fluid. The supersonic object radiates the wake of waves (b), thus its motion deviates from one in a vacuum.

At this point, it is instructive to compare the test particle model of thermal equilibrium to the well-known elementary model of Brownian fluctuations of a particle in a thermally fluctuating fluid. This comparison is given in Table 2.1, below.

Predictably, while there are many similarities between Brownian particles and thermal plasma fluctuations, a key *difference* is that in the case of Brownian motion, the roles of emission and absorption are clearly distinct and played, respectively, by random forces driven by thermal fluctuations in the fluid and by Stokes drag of the fluid on the finite size particle. In contrast, for the plasma the roles of both the emitter and absorber are played by the *plasma particles themselves* in the differing guises of discreteness and as chunks of the Vlasov fluid. In the cases of both the Brownian particle and the plasma, the well-known fluctuation–dissipation theorem of statistical dynamics near equilibrium applies, and relates the fluctuation spectrum to the temperature and the dissipation via the collective mode dissipation, i.e. $\mathrm{Im}\,\epsilon(k,\omega)$, the imaginary part of the collective response function.

Table 2.1. *Comparison of Brownian particle motion and plasma fluctuations*

	Brownian motion	Equilibrium plasma
Excitation	$v_\omega \rightarrow$ velocity mode	$E_{k,\omega} \rightarrow$ Langmuir wave mode
Fluctuation spectrum	$\langle \tilde{v}^2 \rangle_\omega$	$\langle E^2 \rangle_{k,\omega}$
Emission noise	$\langle \tilde{a}^2 \rangle_\omega \rightarrow$ random acceleration by thermal fluctuations	$4\pi q \delta(x - x(t)) \rightarrow$ particle discreteness source
Absorption	Stokes drag on particle	$\mathrm{Im}\,\epsilon \rightarrow$ Landau damping of collective modes
Governing equations	$\frac{d\tilde{v}}{dt} + \beta \tilde{v} = \tilde{a}$	$\nabla \cdot \boldsymbol{D} = 4\pi q \delta(x - x(t))$

2.2.2 *Fluctuation spectrum*

Having discussed the essential physics of the TPM and having identified the dressed test particle as the quasi-particle of interest for the dynamics of near-equilibrium plasma, we now proceed to calculate the plasma fluctuation spectrum near thermal equilibrium. We also show that this spectrum is that required to satisfy the fluctuation–dissipation theorem (F–DT). Subsequently, we use the spectrum to calculate plasma relaxation.

2.2.2.1 *Coherent response and particle discreteness noise*

As discussed above, the central tenets of the TPM are that each particle is both a discrete emitter as well as a participant in the screening or dressing cloud of other particles and that the fluctuations are *weak*, so that linear response theory applies. Thus, the total phase space fluctuation δf is written as

$$\delta f = f^{\mathrm{c}} + \tilde{f}, \tag{2.1}$$

where f^{c} is the coherent Vlasov response to an electric field fluctuation, i.e.

$$f^{\mathrm{c}}_{k,\omega} = R_{k,\omega} E_{k,\omega},$$

where $R_{k,\omega}$ is a linear response function and $\tilde{f}$ is the particle discreteness noise source, i.e.

$$\tilde{f}(x, v, t) = \frac{1}{n} \sum_{i=1}^{N} \delta(x - x_i(t)) \delta(v - v_i(t)) \tag{2.2}$$

(see, Fig. 2.5). For simplicity, we consider high frequency fluctuations in an electron–proton plasma, and assume the protons are simply a static background.

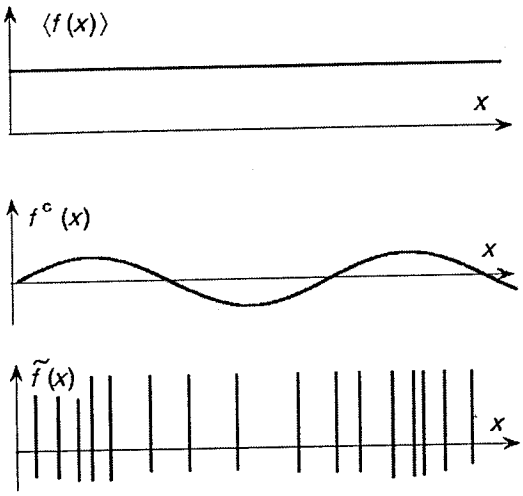

Fig. 2.5. Schematic drawing of the distribution of plasma particles. The distribution function, $f(x, v)$, is divided into the mean $\langle f \rangle$, the coherent response f^c, and the fluctuation part owing to the particle discreteness $\tilde{f}$.

Consistent with linear response theory, we use unperturbed orbits to approximate $x_i(t)$, $v_i(t)$ as:

$$v_i(t) = v_i(0) \tag{2.3a}$$

$$x_i(t) = x_i(0) + v_i t. \tag{2.3b}$$

Since $k_B T \gg q^2/\bar{r}$, the fundamental ensemble here is one of uncorrelated, discrete test particles. Thus, we can define the ensemble average of a quantity A to be

$$\langle A \rangle = n \int \mathrm{d}\boldsymbol{x}_i \int \mathrm{d}\boldsymbol{v}_i \, f_0(\boldsymbol{v}_i, \boldsymbol{x}_i) \, A, \tag{2.4}$$

where $\boldsymbol{x}_i$ and $\boldsymbol{v}_i$ are the phase space coordinates of the particles and f_0 is same near-equilibrium distribution, such as a local Maxwellian. For a Vlasov plasma, which obeys

$$\frac{\partial f}{\partial t} + v\frac{\partial f}{\partial x} + \frac{q}{m}E\frac{\partial f}{\partial v} = 0, \tag{2.5a}$$

the linear response function $R_{k,\omega}$ is

$$R_{k,\omega} = -i\frac{q}{m}\frac{\partial \langle f \rangle / \partial v}{\omega - kv}. \tag{2.5b}$$

Self-consistency of the fields and the particle distribution are enforced by Poisson's equation

$$\nabla^2\phi = -4\pi \sum_s n_s q_s \int \mathrm{d}v\, \delta f_s, \tag{2.6a}$$

so that the potential fluctuation may be written as:

$$\phi_{k,\omega} = -\frac{4\pi n_0 q}{k^2} \int \mathrm{d}v\, \frac{\tilde{f}_{k,\omega}}{\epsilon(k,\omega)}, \tag{2.6b}$$

where the plasma collective response or dielectric function $\epsilon(k,\omega)$ is given by:

$$\epsilon(k,\omega) = 1 + \frac{\omega_p^2}{k} \int \mathrm{d}v\, \frac{\partial \langle f \rangle / \partial v}{\omega - kv}. \tag{2.6c}$$

Note that Eqs.(2.6) relate the fluctuation level to the discreteness noise emission and to $\epsilon(k,\omega)$, the linear collective response function.

2.2.2.2 *Fluctuations driven by particle discreteness noise*

A heuristic explanation is given here that the 'discreteness' of particles induces fluctuations. Consider a case that charged particles (charge q) are moving as shown in Figure 2.6(a). The distance between particles is given by d, and particles are moving at the velocity u. (The train of particles in Fig. 2.6(a) is a part of the distribution of particles. Of course, the net field is calculated by accumulating contributions from all particles.) Charged particles generate the electric field. The time-varying electric field (measured at the position A) is shown in Figure 2.6(b). When we make one particle smaller, but keeping the average density constant, the oscillating field at A becomes smaller. For instance, if the charge of one particle becomes half $q/2$ while the distance between particles is halved, we see that the amplitude of the varying electric field becomes smaller while the frequency becomes higher. This situation is shown in Figure 2.6(b) by a dashed line. In the limit of continuity, i.e.,

Charge per particle $\to 0$
Distance between particle $\to 0$,

while the average density is kept constant, the amplitude of the fluctuating field goes to zero. This example illustrates why 'discreteness' induces fluctuations.

Before proceeding with calculating the spectrum, we briefly discuss an important assumption we have made concerning collective resonances. For a discrete test particle moving on unperturbed orbits,

$$\tilde{f} \sim q\delta(x - x_{0i}(t))\delta(v - v_{0i})$$

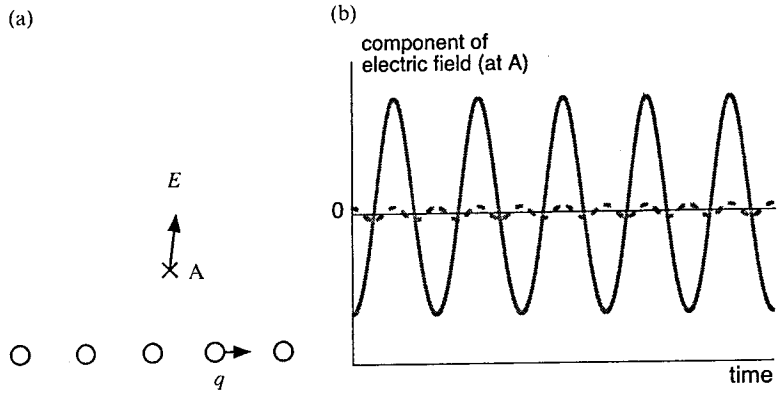

Fig. 2.6. Schematic illustration that the discreteness of particles is the origin of radiations. A train of charged particles (charge q, distance d) is moving near by the observation point A (a). The vertical component of the electric field observed at point A (b). When each particle is divided into two particles, (i.e. charge per particle is $q/2$ and distance between particles is $d/2$), the amplitude of the observed field becomes smaller (dashed curve in (b)).

so

$$\int \mathrm{d}v\, \tilde{f}_k \sim q\mathrm{e}^{-ikvt}$$

and

$$\epsilon(k,t)\phi_k(t) = \frac{4\pi}{k^2} q\mathrm{e}^{-ikvt}.$$

Here, the dielectric is written as an operator ϵ, to emphasize the fact that the response is non-local in time, on account of *memory* in the dynamics. Then strictly speaking, we have

$$\phi_k(t) = \epsilon^{-1} \cdot \left[\frac{4\pi q}{k^2}\mathrm{e}^{-ikvt}\right] + \phi_{k,\omega_k}\mathrm{e}^{-i\omega_k t}. \tag{2.7}$$

In Eq.(2.7), the first term on the right-hand side is the inhomogeneous solution driven by discreteness noise, while the second term is the homogeneous solution (i.e. solution of $\epsilon\phi = 0$), which corresponds to an eigenmode of the system (i.e. a fluctuation at k, ω which satisfies $\epsilon(k,\omega) \simeq 0$, so $\omega = \omega_k$). However, the condition that the plasma be 'near equilibrium' requires that all collective modes be damped (i.e. $\mathrm{Im}\,\omega_k < 0$), so the homogeneous solutions decay in time. Thus, in a near-equilibrium plasma,

$$\phi_k(t) \xrightarrow[t\to\infty]{} \epsilon^{-1} \cdot \left[\frac{4\pi q}{k^2}\mathrm{e}^{-ikvt}\right],$$

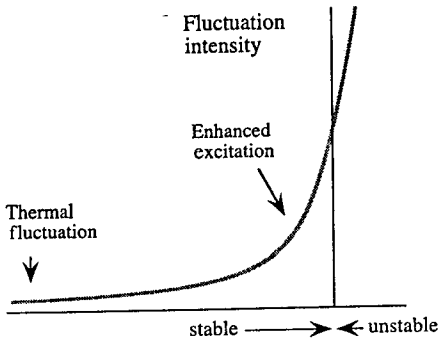

Fig. 2.7. Fluctuation level near the stability boundary. Even if the modes are stable, enhanced excitation of eigenmodes is possible when the controlling parameter approaches the boundary of stability. Linear theory could be violated even if the eigenmodes are stable. Nonlinear noise is no longer negligible.

so only the inhomogeneous solution survives. Two important caveats are necessary here. First, for weakly damped modes with $\mathrm{Im}\,\omega_k \lessapprox 0$, one may need to wait quite a long time indeed to actually arrive at asymptopia. Thus the homogeneous solutions may be important, in practice. Second, for weakly damped ('soft') modes, the inhomogeneous solution $\hat{\phi} \sim |\mathrm{Im}\,\epsilon|^{-1}$ can become large and produce significant orbit scattering and deflection. The relaxation times of such 'soft modes', thus, increase significantly. This regime of approach to marginality from below is analogous to the approach to criticality in a phase transition, where relaxation times and correlation lengths diverge, and fluctuation levels increase. As in the case of critical phenomena, renormalization is required for an accurate theoretical treatment of this regime. The moral of the story related in this small digression is that the TPM's validity actually fails *prior* to the onset of linear instability, rather than *at* the instability threshold, as is frequently stated. The behaviour of fluctuation levels near the stability boundary is schematically illustrated in Figure 2.7. Even if the modes are stable, enhanced excitation of eigenmodes is possible when the controlling parameter is sufficiently close to the boundary of stability, approaching from below. Linear response theory could be violated even if the eigenmodes are stable.

2.2.2.3 *Potential fluctuations*

Proceeding with the calculation of the spectrum, we first define the spectral density of the potential fluctuation as the transform of the potential fluctuation correlation function, i.e.

$$\left\langle \phi^2 \right\rangle_{k,\omega} = \int_{-\infty}^{\infty} \mathrm{d}x \int_{0}^{\infty} \mathrm{d}t\, \mathrm{e}^{i(\omega t - k\cdot x)} \left\langle \phi(0,0)\phi(x,t) \right\rangle \tag{2.8a}$$

and

$$\langle\phi(0,0)\phi(\boldsymbol{x},t)\rangle = \int_{-\infty}^{\infty}\frac{\mathrm{d}\boldsymbol{k}}{(2\pi)^3}\int_{-\infty}^{\infty}\frac{\mathrm{d}\omega}{2\pi}\mathrm{e}^{i(\boldsymbol{k}\cdot\boldsymbol{x}-\omega t)}\left\langle\phi^2\right\rangle_{k,\omega}. \tag{2.8b}$$

Note that the transformation is a Fourier transform in space but a Laplace transform in time. The "one-sided" Laplace transform is intrinsic to fluctuation and TPM theory, as both are built upon the idea of causality, along with assumptions of stationarity and linear response. As linear response theory applies here, the fluctuation modes are uncorrelated, so

$$\left\langle\phi_{k\omega}\phi_{k'\omega'}\right\rangle = (2\pi)^4\left\langle\phi^2\right\rangle_{k,\omega}\delta(\boldsymbol{k}+\boldsymbol{k}')\delta(\omega+\omega'). \tag{2.8c}$$

Therefore, from Eqs.(2.8a)–(2.8c) and Eq.(2.6b), we can immediately pass to the expression for the potential fluctuation spectrum,

$$\left\langle\phi^2\right\rangle_{k,\omega} = \left(\frac{4\pi n_0}{k^2}q\right)^2\int \mathrm{d}v_1\int \mathrm{d}v_2\,\frac{\left\langle\tilde{f}(1)\tilde{f}(2)\right\rangle_{k,\omega}}{|\epsilon(k,\omega)|^2}. \tag{2.9}$$

Here (1) and (2) refer to points in phase space. Observe that the fluctuation spectrum is entirely determined by the discreteness correlation function $\left\langle\tilde{f}(1)\tilde{f}(2)\right\rangle$ and the dielectric function $\epsilon(\boldsymbol{k},\omega)$. Moreover, we know *ab initio* that since the plasma is in equilibrium at temperature T, the fluctuation–dissipation theorem applies, so that the TPM spectrum calculation *must* recover the general ~~F–DT~~ FDT result, which is,

$$\frac{\langle D^2\rangle_{k,\omega}}{4\pi} = \frac{2T}{\omega}\cdot\mathrm{Im}\,\epsilon(k,\omega). \tag{2.10}$$

Here $\boldsymbol{D}_{k,\omega} = \epsilon(k,\omega)\boldsymbol{E}_{k,\omega}$ is the electric displacement vector. Note that the ~~F–DT~~ FDT quite severely constrains the form of the particle discreteness noise.

2.2.2.4 *Correlation of particles and fluctuation spectrum*

To calculate $\left\langle\tilde{f}(1)\tilde{f}(2)\right\rangle_{k,\omega}$, we must first determine $\left\langle\tilde{f}(1)\tilde{f}(2)\right\rangle$. Since $\tilde{f}$ is the distribution of discrete uncorrelated test particles, we have:

$$\tilde{f}(x,v,t) = \frac{1}{n}\sum_{i=1}^{N}\delta(x-x_i(t))\delta(v-v_i(t)). \tag{2.11}$$

From Eqs.(2.3), (2.4) and (2.11), we obtain

$$\left\langle \tilde{f}(1)\tilde{f}(2)\right\rangle = \int \mathrm{d}x_i \int \mathrm{d}v_i \frac{\langle f\rangle}{n} \sum_{i,j=1}^{N} [\delta(x_1 - x_i(t)) \times \delta(x_2 - x_j(t))\delta(v_1 - v_i(t))\delta(v_2 - v_j(t))]. \tag{2.12}$$

Since the product of δs is non-zero only if the arguments are interchangeable, we obtain immediately the discreteness correlation function

$$\left\langle \tilde{f}(1)\tilde{f}(2)\right\rangle = \frac{\langle f\rangle}{n}\delta(x_1 - x_2)\delta(v_1 - v_2). \tag{2.13}$$

Equation (2.13) gives the *discreteness correlation function* in *phase space*. Since the physical model is one of an ensemble of discrete, uncorrelated test particles, it is no surprise that $\left\langle \tilde{f}(1)\tilde{f}(2)\right\rangle$ is *singular*, and *vanishes unless the two points in phase space are coincident*. Calculation of the fluctuation spectrum requires the velocity integrated discreteness correlation function $C(\boldsymbol{k}, \omega)$ which, using spatial homogeneity, is given by:

$$\begin{aligned} C(\boldsymbol{k}, \omega) &= \int \mathrm{d}v_1 \int \mathrm{d}v_2 \left\langle \tilde{f}(1)\tilde{f}(2)\right\rangle_{k,\omega} \\ &= \int \mathrm{d}v_1 \int \mathrm{d}v_2 \left[\int_0^\infty \mathrm{d}\tau\, \mathrm{e}^{i\omega\tau} \int \mathrm{d}x\, \mathrm{e}^{-i\boldsymbol{k}\cdot\boldsymbol{x}} \left\langle \tilde{f}(0)\tilde{f}(\boldsymbol{x}, \tau)\right\rangle \right. \\ &\quad \left. + \int_{-\infty}^0 \mathrm{d}\tau\, \mathrm{e}^{-i\omega\tau} \int \mathrm{d}\boldsymbol{x}\, \mathrm{e}^{-i\boldsymbol{k}\cdot\boldsymbol{x}} \left\langle \tilde{f}(\boldsymbol{x}, -\tau)\tilde{f}(0)\right\rangle \right]. \end{aligned} \tag{2.14}$$

Note that the time history which determines the frequency dependence of $C(\boldsymbol{k}, \omega)$ is extracted by propagating particle (2) *forward* in time and particle (1) *backward* in time, resulting in the *two* Laplace transforms in the expression for $C(\boldsymbol{k}, \omega)$. The expression for $C(\boldsymbol{k}, \omega)$ can be further simplified by replacing v_1, v_2 with $(v_1 \pm v_2)/2$, performing the trivial ~~δ-integration~~, and using unperturbed orbits to obtain

$$\begin{aligned} C(\boldsymbol{k}, \omega) &= 2 \int \mathrm{d}v \int_0^\infty \mathrm{d}\tau\, \mathrm{e}^{i\omega\tau} \int \mathrm{d}x\, \mathrm{e}^{-i\boldsymbol{k}\cdot\boldsymbol{x}} \frac{\langle f(v)\rangle}{n}\delta(x - v\tau) \\ &= 2 \int \mathrm{d}v \frac{\langle f(v)\rangle}{n} \int_0^\infty \mathrm{d}\tau\, \mathrm{e}^{i(\omega - \boldsymbol{k}\cdot v)\tau} \\ &= \int \mathrm{d}v\, 2\pi \frac{\langle f(v)\rangle}{n}\delta(\omega - \boldsymbol{k}\cdot\boldsymbol{v}). \end{aligned} \tag{2.15}$$

Equation (2.15) gives the well-known result for the density fluctuation correlation function in k, ω of an ensemble of discrete, uncorrelated test particles. $C(k, \omega)$ is also the particle discreteness noise spectrum. Note that $C(k, \omega)$ is composed of the unperturbed orbit propagator $\delta(\omega - k \cdot v)$, a weighting function $\langle f \rangle$ giving the distribution of test particle velocities, and the factor of $1/n$, which is a generic measure of discreteness effects. Substitution of $C(k, \omega)$ into Eq.(2.9) then finally yields the explicit general result for the TPM potential fluctuation spectrum:

$$\left\langle \phi^2 \right\rangle_{k,\omega} = \left(\frac{4\pi n_0}{k^2} q \right)^2 \frac{\int \mathrm{d}v \, \frac{2\pi}{n} \langle f \rangle \, \delta(\omega - k \cdot v)}{|\epsilon(k, \omega)|^2}. \tag{2.16}$$

2.2.2.5 *One-dimensional plasma*

In order to elucidate the physics content of the fluctuation spectrum, it is convenient to specialize the discussion to the case of a 1D plasma, for which:

$$C(k, \omega) = \frac{2\pi}{n|k|v_T} F(\omega/k) \tag{2.17a}$$

$$\left\langle \phi^2 \right\rangle_{k,\omega} = n_0 \left(\frac{4\pi q}{k^2} \right)^2 \frac{2\pi}{|k|v_T} \frac{F(\omega/k)}{|\epsilon(k, \omega)|^2}. \tag{2.17b}$$

Here, F refers to the average distribution function, with the normalization factor of v_T extracted, $\langle f(v) \rangle = (n/v_T) F(v)$, and v_T is a thermal velocity. It is interesting to observe that $\langle \phi^2 \rangle_{k,\omega} \sim$ (density) $\times$ (Coulomb spectrum) $\times$ (propagator) $\times$ (particle emission spectrum) $\times$ (screening). Thus, spectral line structure in the TPM is determined by the distribution of Cerenkov emission from the ensemble of discrete particles (set by $\langle f \rangle$) and the collective resonances (where $\epsilon(k, \omega)$ becomes small).

In particular, for the case of an electron plasma with stationary ions, the natural collective mode is the electron plasma wave, with frequency $\omega \simeq \omega_p(1 + \gamma k^2 \lambda_D^2)^{1/2}$ (γ: specific heat ratio of electrons) (Ichimaru, 1973; Krall and Trivelpiece, 1973). So for $\omega \gg \omega_p, k v_T$, $\epsilon \to 1$, we have;

$$\left\langle \phi^2 \right\rangle_{k,\omega} \simeq n_0 \left(\frac{4\pi q}{k^2} \right)^2 \frac{2\pi}{|k|v_T} F(\omega/k), \tag{2.18a}$$

where $F \sim \exp[-\omega^2/k^2 v_T^2]$ for a Maxwellian distribution, while in the opposite limit of $\omega \ll \omega_p, k v_T$ where $\epsilon \to 1 + k^{-2}\lambda_D^{-2}$, the spectrum becomes

$$\left\langle \phi^2 \right\rangle_{k,\omega} \simeq n_0 (4\pi q)^2 \frac{2\pi}{|k|v_T} \left(1 + 1/k^2 \lambda_D^2 \right)^{-2}. \tag{2.18b}$$

In the first, super-celeric limit, the discrete test particle effectively decouples from the collective response, while in the second, quasi-static limit, the spectrum is that of an ensemble of Debye-screened test particles. This region also corresponds to the $k\lambda_{De} \gg 1$ range, where the scales are too small to support collective modes. In the case where collective modes are weakly damped, one can simplify the structure of the screening response via the pole approximation, which is obtained by expanding about ω_k, i.e.

$$\begin{aligned}\epsilon(k,\omega) &= \epsilon_r(k,\omega) + i\,\mathrm{Im}\,\epsilon(k,\omega) \\ &\simeq \epsilon_r(k,\omega_k) + (\omega-\omega_k)\left.\frac{\partial\epsilon}{\partial\omega}\right|_{\omega_k} + i\,\mathrm{Im}\,\epsilon(k,\omega_k). \end{aligned} \tag{2.19}$$

So since $\epsilon_r(k,\omega_k) \approx 0$,

$$\begin{aligned} 1/|\epsilon|^2 &\simeq \frac{1}{|\mathrm{Im}\,\epsilon|}\left\{\frac{|\mathrm{Im}\,\epsilon|}{(\omega-\omega_k)^2|\frac{\partial\epsilon}{\partial\omega}|^2 + |\mathrm{Im}\,\epsilon|^2}\right\} \\ &\simeq \frac{1}{|\mathrm{Im}\,\epsilon|\,|\partial\epsilon_r/\partial\omega|}\cdot\delta(\omega-\omega_k). \end{aligned} \tag{2.20}$$

Here it is understood that $\mathrm{Im}\,\epsilon$ and $\partial\epsilon_r/\partial\omega$ are evaluated at ω_k. Notice that in the pole approximation, eigenmode spectral lines are weighted by the dissipation $\mathrm{Im}\,\epsilon$.

The fluctuation spectrum of plasma oscillations in thermal equailibrium is shown in Figure 2.8. The real frequency and the damping rate of the plasma oscillation are shown as a function of the wavenumber in (a). In the regime of $k\lambda_{De} \ll 1$, the real frequency is close to the plasma frequency, $\omega \sim \omega_p$, and the damping rate is exponentially small. The power spectrum of fluctuations as a function of the frequency is illustrated in (b) for various values of the wave number. In the regime of $k\lambda_{De} \ll 1$, a sharp peak appears near the eigenfrequency $\omega \sim \omega_k$. Owing to the very weak damping, the line width is narrow. As the mode number becomes large (in the regime of $k\lambda_{De} \sim 1$), the bandwidth becomes broader, showing the fact that fluctuations are generated and absorbed very rapidly.

2.2.2.6 *Fluctuation–dissipation theorem and energy partition*

By now, the reader is surely anxious to see if the results obtained using the test particle model are in fact consistent with the requirements and expectations of generalized fluctuation theory, as advertised. First, we check that the fluctuation–dissipation theorem is satisfied. This is most easily accomplished for the case of a Maxwellian plasma. There,

$$\mathrm{Im}\,\epsilon = -\frac{\omega_p^2\pi}{k|k|}\left.\frac{\partial\langle f\rangle}{\partial v}\right|_{\omega/k} = \frac{2\pi\omega}{k^2v_T^2}\frac{\omega_p^2}{|k|v_T}F_M\left(\frac{\omega}{k}\right), \tag{2.21a}$$

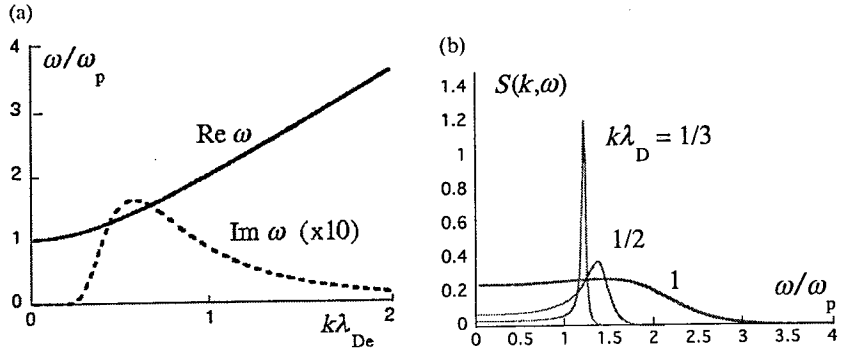

Fig. 2.8. Illustration of the fluctuation spectrum of plasma oscillations. The real frequency and the damping rate of the plasma oscillation are shown as a function of the wavenumber in (a). In the regime of $k\lambda_{De} \ll 1$, $\omega \sim \omega_p$ holds and that the damping rate is exponentially small. The power spectrum of fluctuation as a function of the frequency is illustrated in (b) as a function of the wave number. In the regime of $k\lambda_{De} \ll 1$, a high and sharp peak appears near the eignfrequency $\omega \sim \omega_k$. Owing to the very weak damping, the line width is narrow. As the mode number becomes large an in the regime of $k\lambda_{De} \sim 1$, the bandwidth becomes broader, and the fluctuation intensity becomes high.

so using Eq.(2.21a) to relate $\mathrm{Im}\,\epsilon(k,\omega)$ to $F(\omega/kv_T)$ in Eq.(2.17b) gives

$$\left\langle \phi^2 \right\rangle_{k,\omega} = \frac{8\pi T}{k^2\omega}\frac{\mathrm{Im}\,\epsilon}{|\epsilon|^2}, \tag{2.21b}$$

so we finally obtain

$$\frac{\langle D^2 \rangle_{k,\omega}}{4\pi} = \frac{2T}{\omega}\mathrm{Im}\,\epsilon \tag{2.21c}$$

which is in precise agreement with the statement of the F–DT for a classical, plasma at temperature T. It is important to reiterate here that applicability of the F–DT rests upon to the applicability of linear response theory for the emission and absorption of each mode. Both fail as the instability marginal point is approached (from below).

Second, we also examine the k-spectrum of energy, with the aim of comparing the TPM prediction to standard expectations for thermal equilibrium, i.e. to see whether energy is distributed according to the conventional wisdom of "$T/2$ per degree-of-freedom". To this end, it is useful to write (using Eq.(2.21)) the electric field energy as:

$$\frac{|E_{k,\omega}|^2}{8\pi} = \frac{4\pi n q^2}{k|k|}\left\{\frac{F(\omega/k)}{\left(1-\frac{\omega_p^2}{\omega^2}\right)^2+\left(\frac{\pi\omega_p^2}{k|k|}F'\right)^2}\right\}, \tag{2.22}$$

where $\epsilon_r \simeq 1-\omega_p^2/\omega^2$ for plasma waves, and $F' = \mathrm{d}F/\mathrm{d}u|_{\omega/k}$. The total electric field energy per mode, E_k, is given by

$$E_k = \int \mathrm{d}\omega \, \frac{|E_{k,\omega}|^2}{8\pi}, \tag{2.23a}$$

so that use of the pole approximation to the collective resonance and a short calculation then gives,

$$E_k = \frac{n_e\omega_p}{2|k|}\frac{F}{|F'|} = \frac{T}{2}. \tag{2.23b}$$

So, yes, the electric field energy for plasma waves is indeed equipartioned! Since for plasma waves the particle kinetic energy density E_{kin} equals the electric field energy density E_k (i.e. $E_{\mathrm{kin}} = E_k$), the total wave energy density per mode W_k is constant at T. Note that Eq.(2.23b) does not imply the divergence of total energy density. Of course, some fluctuation energy is present at very small scales ($k\lambda_{\mathrm{De}} \gtrsim 1$) which cannot support collective modes. However, on such scales, the pole expansion is not valid and simple static screening is a better approximation. A short calculation gives, for $k^2\lambda_{\mathrm{De}}^2 > 1$, $E_k \cong (T/2)/k^2\lambda_{\mathrm{De}}^2$, so that the *total* electric energy density is

$$\left\langle\frac{E^2}{8\pi}\right\rangle = \int \mathrm{d}k\, E_k$$
$$= \int_{-\infty}^{\infty}\frac{\mathrm{d}k}{2\pi}\frac{T/2}{(1+k^2\lambda_{\mathrm{De}}^2)} \sim \left(\frac{nT}{2}\right)\left(\frac{1}{n\lambda_{\mathrm{De}}}\right). \tag{2.24}$$

As Eq.(2.24) is for 1D, there n has the dimensions of particles-per-distance. In 3D, the analogue of this result is

$$\left\langle\frac{E^2}{8\pi}\right\rangle \sim \left(\frac{nT}{2}\right)\left(\frac{1}{n\lambda_{\mathrm{De}}^3}\right), \tag{2.25}$$

so that the total electric field energy equals the total thermal energy times the discreteness factor $1/n\lambda_{\mathrm{De}}^3 \sim 1/N$, where N is the number of particles in a Debye sphere. Hence $\langle E^2/8\pi\rangle \ll nT/2$, as is required for a plasma with weak correlations.

2.2.3 Relaxation near equilibrium and the Balescu–Lenard equation

Having determined the equilibrium fluctuation spectrum using the TPM, we now turn to the question of how to *use it to calculate relaxation near equilibrium.* By "relaxation" we mean the long time evolution of the mean (i.e. ensemble averaged) distribution function $\langle f \rangle$. Here 'long time' means long or slow evolution in comparison to fluctuation time scales. Generally, we expect the mean field equation for the prototypical example of a 1D electrostatic plasma to have the form of a continuity equation in velocity space, i.e.

$$\frac{\partial \langle f \rangle}{\partial t} = -\frac{\partial}{\partial v} J(v). \tag{2.26}$$

Here, $J(v)$ is a flux or current and $\langle f \rangle$ is the corresponding coarse-grained phase space density; $J \xrightarrow[v \to \pm\infty]{} 0$ assures conservation of total $\langle f \rangle$. *The essence of the problem* at hand is *how to actually calculate* $J(v)$! Of course it is clear from the Vlasov equation that $J(v)$ is simply the average acceleration $\langle (q/m) E \delta f \rangle$ due to the phase space density fluctuation δf. Not surprisingly, then, $J(v)$ is most directly calculated using a mean field approach. Specifically, simply substitute the *total* δf into $\langle (q/m) E \delta f \rangle$ to calculate the current $J(v)$. Since $\delta f = f^c + \tilde{f}$, $J(v)$ will necessarily consist of *two* pieces. The *first piece*, $\langle (q/m) E f^c \rangle$, accounts for the *diffusion in velocity* driven by the TPM potential fluctuation spectrum. This contribution can be obtained from a Fokker–Planck calculation using the TPM spectrum as the noise. The *second piece*, $\left\langle (q/m) E \tilde{f} \right\rangle$, accounts for relaxation driven by the *dynamic friction* between the ensemble of discrete test particles and the Vlasov fluid. It accounts for the evolution of $\langle f \rangle$ which must accompany the slowing down of a test particle by wave drag. The second piece has the structure of a drag term. As is shown in the derivation of Eq.(2.16), $\langle E f^c \rangle$ ultimately arises from the discreteness of particles, $\tilde{f}_1$.

The kinetic equation for $\langle f \rangle$ which results from this mean field calculation was first derived by R. Balescu and A. Lenard, and so is named in their honour (Lenard, 1960; Balescu, 1963). The diffusion term of the Balescu–Lenard (B–L) equation is very similar to the quasi-linear diffusion operator, discussed in Chapter 3, although the electric field fluctuation spectrum is prescribed by the TPM and the frequency spectrum is not restricted to eigenmode frequency lines, as in the quasi-linear theory. The total phase space current $J(v)$ is similar in structure to that produced by the glancing, small angle Coulomb interactions which the Landau collision integral calculates. (See Rosenbluth *et al.* (1957), Rostoker and Rosenbluth (1960) and Ichimaru and Rosenbluth (1970) for the Fokker–Planck approach to Coulomb collisions.) However, in contrast to the Landau theory, the B–L equation incorporates *both* static and dynamic screening, and so treats the interaction of collective

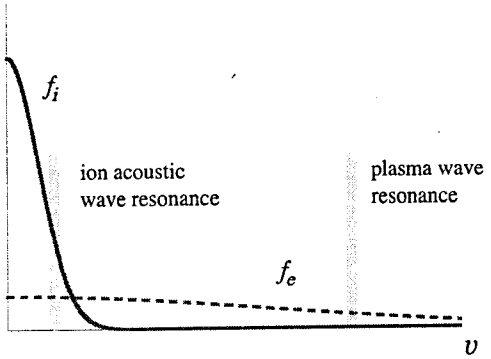

Fig. 2.9. Structure of $\langle f_i \rangle$, $\langle f_e \rangle$ for stable plasma. Velocity space configuration, showing electron plasma wave resonance on the tail of f_e and ion acoustic wave resonance in the bulk of f_e, f_i. In the case with $T_e \gg T_i$, waves can resonate with the bulk of the electron distribution while avoiding ion Landau damping. The slope of f_e is small at resonance, so ion acoustic waves are only weakly damped. In the case with $T_e \sim T_i$, ion acoustic waves resonant in the bulk of f_e cannot avoid ion Landau damping, so the collective modes are heavily damped.

processes with binary encounters. Screening also eliminates the divergences in the Landau collision integral (i.e. the Coulomb logarithm) which are due to long range electrostatic interactions. Like the Landau integral, the B–L equation is ultimately *nonlinear* in $\langle f \rangle$.

At this point, the sceptical reader will no doubt be entertaining question like, "What kind of relaxation is possible here?", "how does it differ from the usual collisional relaxation process?" and "just what, precisely, does 'near equilibrium' mean?". One point relevant to all these questions is that it is easy to define states that have finite free energy, but which are *stable* to collective modes. One example is the current-driven ion acoustic (CDIA) system shown in Figure 2.9. Here the non-zero current, which shifts the electron Maxwellian, constitutes free energy. However, since the shift does not produce a slope in $\langle f_e \rangle$ sufficient to overcome ion Landau damping, the free energy is *not* accessible to linear CDIA instabilities (Ichimaru, 1973). Nevertheless, electron $\rightarrow$ ion momentum transfer *is* possible, and *can* result in electron relaxation, since the initial state is *not* one of maximum entropy. Here, relaxation occurs via binary interactions of *dressed* test particles. Note however, that in this case relaxation rates may be significantly faster than for 'bare' particle collisions, on account of fluctuation enhancement by weakly damped collective modes. Thus, the B–L theory offers both something old and something new relative to its collisional antecedent, the Landau theory.

In order to best elucidate the physics of relaxation processes, we keep the calculations as simple as possible and divide our discussion into three parts. The basic

theory is developed for an electrostatic plasma in one dimension, and then applied to single species and two species relaxation processes. Single species relaxation in 3D is then considered followed by a discussion of collective enhancement of momentum exchange.

2.2.3.1 Kinetic equation for mean distribution function

The Balescu–Lenard equation may be derived by a mean-field calculation of the fluctuation-induced acceleration $(q/m)\langle E\delta f\rangle$. Specifically,

$$\begin{aligned}\frac{\partial \langle f\rangle}{\partial t} &= -\frac{\partial}{\partial v}\frac{q}{m}\langle E\delta f\rangle \\ &= -\frac{\partial}{\partial v}J(v),\end{aligned} \tag{2.27}$$

where $J(v)$ must be calculated using the *total* δf, which includes both the linear response f^{c} and the discreteness fluctuation $\tilde{f}$. Thus, substitution of

$$\delta f = f^{\mathrm{c}} + \tilde{f},$$

yields

$$\begin{aligned}J(v) &= -\left(\frac{q}{m}\langle Ef^{\mathrm{c}}\rangle + \frac{q}{m}\left\langle E\tilde{f}\right\rangle\right) \\ &= -D(v)\frac{\partial \langle f\rangle}{\partial v} + F_f(v),\end{aligned} \tag{2.28}$$

where $D(v)$ is the fluctuation-induced diffusion, while $F_f(v)$ is the dynamical friction term. Consistent with linear response theory, we can then write:

$$f^{\mathrm{c}}_{k,\omega} = -i\frac{(q/m)E_{k,\omega}}{\omega - kv}\frac{\partial \langle f\rangle}{\partial v}. \tag{2.29a}$$

so for stationary fluctuations, a short calculation gives:

$$D(v) = \sum_{k,\omega}\frac{q^2}{m^2}k^2\left\langle\phi^2\right\rangle_{k,\omega}\pi\delta(\omega - kv). \tag{2.29b}$$

The spectrum $\langle\phi^2\rangle_{k,\omega}$ is understood to be the test particle model spectrum, i.e. that of Eq.(2.17b). Similarly, the dynamical friction term $F_f(v)$ is given by

$$F_f(v) = -\frac{q}{m}\sum_{k,\omega} ik\left\langle\phi\tilde{f}\right\rangle_{k,\omega}, \tag{2.30a}$$

where, via Eq.(2.6b), we have:

$$\left\langle \phi \tilde{f} \right\rangle_{k,\omega} = \frac{4\pi n_0 q}{k^2} \int \mathrm{d}v \, \frac{\left\langle \tilde{f} \tilde{f} \right\rangle_{k,\omega}}{\epsilon(k,\omega)^*}. \tag{2.30b}$$

This result explains that the discreteness of particles is the source of correlations in the excited mode. Since

$$\left\langle \phi^2 \right\rangle_{k,\omega} = \left(\frac{4\pi n_0 q}{k^2} \right)^2 \frac{C(k,\omega)}{|\epsilon(k,\omega)|^2},$$

and (from Eq.(2.14))

$$C(k,\omega) = \left\langle \tilde{n}^2 \right\rangle_{k,\omega} = \int \mathrm{d}v \, 2\pi\delta(\omega - kv) \, \langle f(v) \rangle ,$$

we have

$$\left\langle \phi \tilde{f} \right\rangle_{k,\omega} = \left(\frac{4\pi n_0 q}{k^2} \right) \frac{2\pi\delta(\omega - kv) \, \langle f \rangle}{\epsilon(k,\omega)^*}.$$

Thus, the current $J(v)$ is given by:

$$\begin{aligned} J(v) &= -D(v) \frac{\partial \langle f \rangle}{\partial v} + F_r(v) \\ &= -\sum_{k,\omega} \left(\frac{4\pi n_0 q}{k^2} \right) \frac{q}{m} \left(\frac{2\pi\delta(\omega - kv)}{n_0 |\epsilon(k,\omega)|^2} \right) k \\ &\quad \times \left\{ \left(\frac{4\pi n_0 q}{k^2} \right) \frac{\pi k}{|k| v_{\mathrm{T}}} \left(\frac{q}{m} \right) F\left(\frac{\omega}{k} \right) \frac{\partial \langle f \rangle}{\partial v} + \mathrm{Im}\, \epsilon(k,\omega) \, \langle f \rangle \right\}. \end{aligned} \tag{2.31}$$

Note that the contributions from the diffusion $D(v)$ and dynamical friction $F_f(v)$ have been grouped together within the brackets. Poisson's equation relates $\epsilon(k,\omega)$ to the electron and ion susceptibilities $\chi(k,\omega)$ by

$$\epsilon(k,\omega) = 1 + \left(\frac{4\pi n_0 q}{k^2} \right) \left[\chi_{\mathrm{i}}(k,\omega) - \chi_{\mathrm{e}}(k,\omega) \right],$$

where χ_{i}, χ_{e} are the ion and electron susceptibilities defined by

$$n_{k,\omega} = \chi_{\mathrm{i}}(k,\omega) \phi_{k,\omega}.$$

It is straightforward to show that

$$\mathrm{Im}\, \epsilon(k,\omega) = -\frac{\pi \omega_{\mathrm{p}}^2}{k^2} \frac{k}{|k| v_{\mathrm{T}}} F'(\omega/k) + \mathrm{Im}\, \epsilon_{\mathrm{i}}(k,\omega), \tag{2.32a}$$

where

$$\mathrm{Im}\,\epsilon_{\mathrm{i}}(k,\omega) = \frac{4\pi n_0 q}{k^2}\mathrm{Im}\,\chi_{\mathrm{i}}(k,\omega). \tag{2.32b}$$

Here $\epsilon_{\mathrm{i}}(k,\omega)$ is the *ion* contribution to the dielectric function. Thus, we finally obtain a simplified expression for $J(v)$:

$$J(v) = -\sum_{k,\omega}\left(\frac{\omega_{\mathrm{p}}^2}{k^2}\right)^2\left(\frac{2\pi^2}{n_0 k v_{\mathrm{T}}}\right)\frac{\delta(\omega - kv)}{|\epsilon(k,\omega)|^2}$$
$$\times\left\{F\left(\frac{\omega}{k}\right)\frac{\partial\langle f\rangle}{\partial v} - \langle f(v)\rangle F'\left(\frac{\omega}{k}\right) + \mathrm{Im}\,\epsilon_{\mathrm{i}}(k,\omega)\langle f\rangle\right\}. \tag{2.33}$$

Equation (2.33) gives the *general* form of the velocity space electron current in the B–L equation for electron relaxation, as described within the framework of the TPM.

In order to elucidate the physics content of $J(v)$, it is instructive to re-write Eq.(2.33) in alternative forms. One way is to define the fluctuation phase velocity by $u = \omega/k$, so that

$$J(v) = -\sum_{k,\omega}\left(\frac{\omega_{\mathrm{p}}^2}{k^2}\right)^2\left(\frac{2\pi^2}{n_0 k v_{\mathrm{T}}}\right)\frac{\delta(u - v)}{|k||\epsilon(k,\omega)|^2}$$
$$\times\left\{F(u)\langle f(v)\rangle' - F'(u)\langle f(v)\rangle + \mathrm{Im}\,\epsilon_{\mathrm{i}}(k,\omega)\langle f(v)\rangle\right\}. \tag{2.34}$$

Alternatively, one could just perform the summation over frequency to obtain

$$J(v) = -\sum_{k}\left(\frac{\omega_{\mathrm{p}}^2}{k^2}\right)^2\left(\frac{\pi}{n_0 k v_{\mathrm{T}}}\right)\frac{1}{|\epsilon(k,kv)|^2}$$
$$\times\left\{F(v)\frac{\partial\langle f(v)\rangle}{\partial v} - \langle f(v)\rangle F'(v) + \mathrm{Im}\,\epsilon_{\mathrm{i}}(k,kv)\langle f(v)\rangle\right\}. \tag{2.35}$$

Finally, it is also useful to remind the reader of the counterpart of Eq.(2.33) in the unscreened Landau collision theory, which we write for 3D as:

$$J_\alpha(\boldsymbol{p}) = -\sum_{\mathrm{e,i}}\int_{q_\alpha}\mathrm{d}^3q\int\mathrm{d}^3p'\,W(\boldsymbol{p},\boldsymbol{p}',\boldsymbol{q})q_\alpha q_\beta\left\{f(\boldsymbol{p}')\frac{\partial f(\boldsymbol{p})}{\partial \boldsymbol{p}_\beta} - \frac{\partial f(\boldsymbol{p}')}{\partial \boldsymbol{p}'_\beta}f(\boldsymbol{p})\right\}. \tag{2.36}$$

In Eq.(2.36), $W(\boldsymbol{p},\boldsymbol{p}',\boldsymbol{q})$ is the transition probability for a collision (with momentum transfer $\boldsymbol{q}$) between a 'test particle' of momentum $\boldsymbol{p}$ and a 'field particle' of momentum $\boldsymbol{p}'$. Here the condition $|\boldsymbol{q}| \ll |\boldsymbol{p}|, |\boldsymbol{p}|'$ applies, since long range Coulomb collisions are 'glancing'.

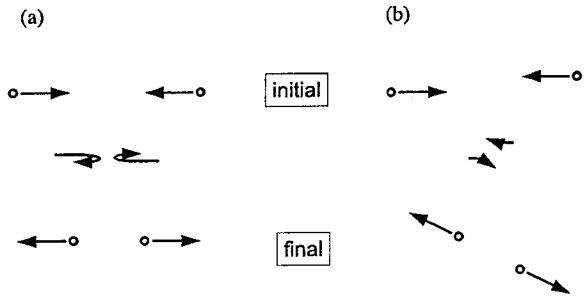

Fig. 2.10. Like-particle collisions in (a) 1D and (b) 3D.

2.2.3.2 *Offset on Landau–Rosenbluth theory*

Several features of $J(v)$ are readily apparent. First, just as in the case of the Landau theory, the current $J(v)$ can be written as a sum of electron–electron and electron–ion scattering terms, i.e.

$$J(v) = -\left[D_{e,e}(v)\frac{\partial \langle f \rangle}{\partial v} + F_{e,e}(v) + F_{e,i}(v)\right]. \tag{2.37}$$

Here $D_{e,e}(v)$ refers to the diffusion (in velocity) of electrons by fluctuations excited by electron discreteness emission, $F_{e,e}(v)$ is the dynamical friction on electrons due to fluctuations generated by discreteness, while $F_{e,i}$ is the electron–ion friction produced by the coupling of emission (again due to electron discreteness) to dissipative ion absorption. Interestingly, in 1D,

$$-D_{e,e}(v)\frac{\partial \langle f \rangle}{\partial v} + F_{e,e}(v) \sim \delta(u - v)\{-F(u)\langle f \rangle' + F'\langle f \rangle\} = 0,$$

since $F = \langle f \rangle$ for single species interaction. Thus, we see that *electron–electron friction exactly cancels electron diffusion in 1D*. In this case,

$$J(v) \sim \delta(u - v)\mathrm{Im}\,\epsilon_i(k, \omega)\langle f_e(v) \rangle,$$

so that electron relaxation is determined *solely* by electron–ion friction. This result is easily understood from consideration of the analogy between same-species interaction in a stable, 1D plasma and like-particle collisions in 1D (Figure 2.10). On account of conservation of energy and momentum, it is trivial to show that such collisions leave final state = initial state, so no entropy production is possible and no relaxation can occur. This fact is manifested in the B–L theory by the cancellation between electron–electron terms – since the only way to produce finite momentum transfer in 1D is via inter-species collisions, the only term that survives in $J(v)$ is $F_{e,i}(v)$. Note that this result is not a purely academic consideration, since a strong magnetic field $\boldsymbol{B}_0$ often imposes a 1D structure on the wave–particle resonance interaction in more complicated problems.

Table 2.2. *Comparison of Landau and Balescu–Lenard relaxation theory*

	Laudau theory	B–L theory
Physical scenario	'Test' particle scattered by distribution of 'field' particles	Test particle scattered by distribution of fluctuations with $v_{ph} = \omega/k$, produced via discreteness
Scatterer distribution	$f(p')$ Field particles distribution	$F(u),\ u = \omega/k$ Fluctuation phase velocity distribution
Correlation	Uncorrelated particles as assumed molecular chaos $\langle f(1,2)\rangle = \langle f(1)\rangle \langle f(2)\rangle$	Discrete uncorrelated test particles $\langle \tilde{f}\tilde{f}\rangle = (\langle f\rangle/n)\delta(x_-)\delta(v_-)$
Screening	None Coulomb $\ln\Lambda$ factor put in 'by intuition'	$1/\lvert\epsilon(k,\omega)\rvert^2$
Scattering strength	$\lvert q\rvert \ll \lvert p\rvert$ Weak deflection	Linear response and unperturbed orbits
Interaction selection Rule	$W(p, p', q) = \delta(p - p')$ in 1D, 1 species	$\delta(u - v)$ in 1D $\delta(k \cdot (v - v'))$ in 3D

A detailed comparison and contrast between the Landau theory of collisions and the B–L theory of near-equilibrium relaxation is presented in Table 2.2.

2.2.3.3 *Resistivity (relaxation in one-dimensional system)*

Having derived the expression for $J(v)$, it can then be used to calculate transport coefficients and to macroscopically characterize relaxation. As an example, we consider the effective resistivity associated with the current driven system of Figure 2.9. To construct an effective Ohm's law for this system, we simply write

$$\frac{\partial \langle f\rangle}{\partial t} + \frac{q}{m}E_0 \frac{\partial \langle f\rangle}{\partial v} = -\frac{\partial J(v)}{\partial v}, \tag{2.38a}$$

and then multiply by $n_0 q v$ and integrate to obtain, in the stationary limit,

$$\begin{aligned} E_0 &= -\frac{4\pi n_0 q}{\omega_p^2}\int dv\, J(v) \\ &= 4\pi n_0 |q| \sum_{k,\omega} \frac{\omega_p^2}{(k^2)^2}\frac{(2\pi/|k|)}{n_0 k v_T}\left(\frac{\operatorname{Im}\epsilon_i(k,\omega)}{|\epsilon(k,\omega)|^2}\right)\left\langle f_e\left(\frac{\omega}{k}\right)\right\rangle \\ &\equiv \eta_{\text{eff}} J_0. \end{aligned} \tag{2.38b}$$

Not surprisingly, the response of $\langle f_e \rangle$ to E_0 cannot unambiguously be written as a simple, constant effective resistivity, since the resonance factor $\delta(\omega - kv)$ and the k, ω dependence of the TPM fluctuation spectrum conflate the field particle distribution function with the spectral structure. However, the necessary dependence of the effective resistivity on electron–ion interaction *is* readily apparent from the factor of $\mathrm{Im}\,\epsilon_i(k, \omega)$. In practice, a non-trivial effect here requires a finite, but not excessively strong, overlap of electron and ion distributions. Note also that collective enhancement of relaxation below the linear instability threshold *is* possible, should $\mathrm{Im}\,\epsilon(k, \omega)$ become small.

2.2.3.4 Relaxation in three-dimensional system

Having discussed the 1D case at some length, we now turn to relaxation in 3D (Lifshitz and Pitaevskii, 1981). The principal effect of three dimensionality is to relax the tight link between particle velocity $\boldsymbol{v}$ and fluctuation phase velocity $(\omega/|k|)\hat{k}$. Alternatively put, conservation constraints on like-particle collisions in 1D force the final state = initial state, but in 3D, glancing collisions which conserve energy and the magnitude of momentum $|\boldsymbol{p}|$, but change the particle's directions, are possible. The contrast between 1D and 3D is illustrated in Figure 2.10. In 3D, the discreteness correlation function is

$$C(k, \omega) = \langle \tilde{n}\tilde{n} \rangle_{k,\omega} = \int \mathrm{d}^3 v \frac{2\pi}{n_0} \delta(\omega - \boldsymbol{k} \cdot \boldsymbol{v}) \langle f \rangle . \tag{2.39}$$

So the B–L current $\boldsymbol{J}(\boldsymbol{v})$ for like-particle interactions becomes

$$\begin{aligned} \boldsymbol{J}(\boldsymbol{v}) = -\sum_{\mathbf{k},\omega} \left(\frac{\omega_\mathrm{p}^2}{k^2}\right)^2 & \frac{2\pi^2 \delta(\omega - \boldsymbol{k} \cdot \boldsymbol{v})}{v_\mathrm{T} n_0 |\epsilon(k, \omega)|^2} \\ & \times \boldsymbol{k} \left\{ \int \mathrm{d}\boldsymbol{v}' \, \delta(\omega - \boldsymbol{k} \cdot \boldsymbol{v}') \left\langle f(\boldsymbol{v}') \right\rangle \boldsymbol{k} \cdot \frac{\partial \langle f \rangle}{\partial \boldsymbol{v}} \right. \\ & \left. - \int \mathrm{d}\boldsymbol{v}' \, \delta(\omega - \boldsymbol{k} \cdot \boldsymbol{v}') \boldsymbol{k} \cdot \frac{\partial \langle f \rangle}{\partial \boldsymbol{v}'} \langle f(\boldsymbol{v}) \rangle \right\}. \end{aligned} \tag{2.40a}$$

Note that the product of delta functions can be re-written as

$$\delta(\omega - \boldsymbol{k} \cdot \boldsymbol{v}) \delta(\omega - \boldsymbol{k} \cdot \boldsymbol{v}') = \delta(\omega - \boldsymbol{k} \cdot \boldsymbol{v}) \delta(\boldsymbol{k} \cdot \boldsymbol{v} - \boldsymbol{k} \cdot \boldsymbol{v}').$$

We thus obtain an alternate form for $\boldsymbol{J}(\boldsymbol{v})$, which is

$$J(v) = -\sum_{\mathbf{k},\omega}\left(\frac{\omega_p^2}{k^2}\right)^2 \frac{2\pi^2\delta(\omega - \boldsymbol{k}\cdot\boldsymbol{v})}{v_T n_0 |\epsilon(k,\omega)|^2}$$
$$\times\left\{\boldsymbol{k}\int \mathrm{d}\boldsymbol{v}'\,\delta(\boldsymbol{k}\cdot\boldsymbol{v} - \boldsymbol{k}\cdot\boldsymbol{v}')\left[\left\langle f(v')\right\rangle \boldsymbol{k}\cdot\frac{\partial\langle f\rangle}{\partial \boldsymbol{v}} - \boldsymbol{k}\cdot\frac{\partial\langle f\rangle}{\partial \boldsymbol{v}'}\langle f(v)\rangle\right]\right\}. \tag{2.40b}$$

This form illustrates an essential aspect of 3D, which is that *only the parallel (to k) components of test and field particle velocities* $\boldsymbol{v}$ and $\boldsymbol{v}'$ *need be equal for interaction to occur*. This is in distinct contrast to the case of 1D, where *identity*, i.e. $v = v' = u$, is required for interaction. Thus, relaxation by like-particle interaction is possible, and calculations of transport coefficients are possible, following the usual procedures of the Landau theory.

2.2.3.5 Dynamic screening

We now come to our final topic in B–L theory, which is *dynamic screening*. It is instructive and enlightening to develop this topic from a direction slightly different from that taken by our discussion up till now. In particular, we will proceed from the Landau theory, but will calculate momentum transfer *including* screening effects and thereby arrive at a B–L equation.

2.2.3.6 Relaxation in Landau model

Starting from Eq.(2.36), the Landau theory expression for the collision-induced current (in velocity) may be written as:

$$J_\alpha(\boldsymbol{p}) = \sum_{\text{species}}\int \mathrm{d}^3p'\left[f(\boldsymbol{p})\frac{\partial f(\boldsymbol{p}')}{\partial \boldsymbol{p}'_\beta} - f(\boldsymbol{p}')\frac{\partial f(\boldsymbol{p})}{\partial \boldsymbol{p}_\beta}\right]B_{\alpha,\beta}, \tag{2.41a}$$

where

$$B_{\alpha,\beta} = \frac{1}{2}\int \mathrm{d}\sigma\, q_\alpha q_\beta |\boldsymbol{v} - \boldsymbol{v}'|. \tag{2.41b}$$

The notation here is standard: $\mathrm{d}\sigma$ is the differential cross-section and $\boldsymbol{q}$ is the momentum transfer in the collision. We will calculate $B_{\alpha,\beta}$ directly, using the same physics assumptions as in the TPM. A background or 'field' particle with velocity $\boldsymbol{v}'$, and charge e' produces a potential field

$$\phi_{k,\omega} = \frac{4\pi e'}{k^2\epsilon(k,\omega)}2\pi\delta(\omega - \boldsymbol{k}\cdot\boldsymbol{v}'), \tag{2.42a}$$

so converting the time transform gives

$$\phi_k(t) = \frac{4\pi e'}{k^2\epsilon(\boldsymbol{k},\boldsymbol{k}\cdot\boldsymbol{v}')}\mathrm{e}^{-i\boldsymbol{k}\cdot\boldsymbol{v}'t}. \tag{2.42b}$$

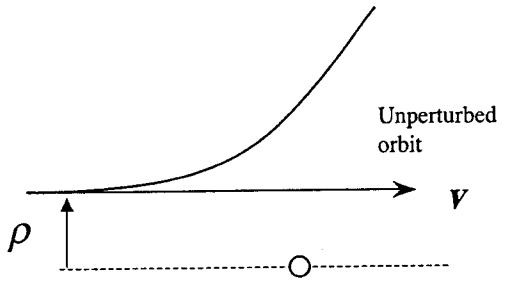

Fig. 2.11. Deflection orbit and unperturbed orbit.

From this, it is straightforward to calculate the net deflection or momentum transfer q by calculating the impulse delivered to a test particle with charge e moving along an unperturbed trajectory of velocity v. This impulse is:

$$q = -\int_{r=\rho+vt} \frac{\partial V}{\partial r} \mathrm{d}t, \tag{2.43a}$$

where the potential energy V is just

$$\begin{aligned} V &= e\phi \\ &= 4\pi ee' \int \mathrm{d}^3k \, \frac{\mathrm{e}^{ik\cdot r}\mathrm{e}^{-ik\cdot v't}}{k^2\epsilon(k, k\cdot v')}. \end{aligned} \tag{2.43b}$$

Here ρ is the impact parameter for the collision, a representation of which is sketched in Figure 2.11. A short calculation then gives the net momentum transfer q,

$$\begin{aligned} q &= 4\pi ee' \int \frac{\mathrm{d}^3k}{(2\pi^3)} \, \frac{-ik\mathrm{e}^{ik\cdot\rho}\, 2\pi\delta(k\cdot(v-v'))}{k^2\epsilon(k, k\cdot v')} \\ &= 4\pi ee' \int \frac{\mathrm{d}^2k_\perp}{(2\pi^3)} \frac{-ik_\perp \mathrm{e}^{ik_\perp\cdot\rho}}{k^2\epsilon(k, k\cdot v')|v-v'|}. \end{aligned} \tag{2.44}$$

To obtain Eq.(2.44), we use

$$\delta(k\cdot(v-v')) = \frac{\delta(k_\parallel)}{|v-v'|},$$

and the directions $\parallel$ and $\perp$ are defined relative to the direction of $v - v'$. Since $J \sim \rho^2$, we may write $B_{\alpha,\beta}$ as,

$$B_{\alpha,\beta} = \int \mathrm{d}^2\rho \, q_\alpha q_\beta |v-v'|. \tag{2.45}$$

Noting that the $d^2\rho$ integration just produces a factor of $(2\pi)^2\delta\left(k_\perp + k'_\perp\right)$, we can then immediately perform one of the $\int d^2k_\perp$ integrals in $B_{\alpha,\beta}$ to get,

$$B_{\alpha,\beta} = 2e^2e'^2 \int d^2k_\perp \frac{k_{\perp\alpha}k_{\perp\beta}}{|k_\perp^2\epsilon(k, k\cdot v')|^2|v - v'|}. \tag{2.46}$$

It is easy to see that Eq.(2.46) for $B_{\alpha,\beta}$ (along with Eq.(2.41a)) is entirely equivalent to the B–L theory for $J(v)$. In particular, note the presence of the dynamic screening factor $\epsilon(k, k\cdot v')$. If screening is neglected, $\epsilon \to 1$ and

$$B_{\alpha,\beta} \sim \int d^2k_\perp \frac{k_\perp^2}{|\epsilon|k_\perp^4} \sim \int dk_\perp/k_\perp \sim \ln(k_{\perp\max}/k_{\perp\min}),$$

which is the familiar Coulomb logarithm from the Landau theory. Note that if $\mathbf{k}, \omega \to 0$,

$$k_\perp^2\epsilon \sim k_\perp^2 + 1/\lambda_D^2,$$

so that Debye screening eliminates the long-range divergence (associated with $k_{\perp\min}$) without the need for an ad hoc factor. To make the final step toward recovering the explicit B–L result, one can 'undo' the $dk_\parallel$ integration and the frequency integration to find,

$$B_{\alpha,\beta} = 2(ee')^2 \int_{-\infty}^{\infty} d\omega \int_{k<k_{\max}} d^3k\, \delta(\omega - k\cdot v)\delta(\omega - k\cdot v')\frac{k_\alpha k_\beta}{k^4|\epsilon(k,\omega)|^2}. \tag{2.47}$$

Here $k_{\max}$ is set by the distance of closest approach, i.e.

$$k_{\max} \sim \frac{\mu v_{\rm rel}^2}{2ee'}.$$

Substituting Eq.(2.47) for $B_{\alpha,\beta}$ into Eq.(2.41a) recovers Eq.(2.40a). This short digression convincingly demonstrates the equivalence of the B–L theory to the Landau theory with dynamic screening.

2.2.3.7 Collective mode

We now explore the enhancement of relaxation by weakly damped collective modes. Consider a stable, two species plasma with electron and ion distribution functions, as shown in Figure 2.9. This plasma has no free energy (i.e. no net current), but is not necessarily a maximum entropy state, if $T_e \neq T_i$. Moreover, the plasma supports two types of collective modes, namely

(i) electron plasma waves, with $v_{Te} < \omega/k$.
(ii) ion acoustic waves, with $v_{Ti} < \omega/k < v_{Te}$,

where v_{Te} and v_{Ti} are the electron and ion thermal speeds, respectively. Electron plasma waves are resonant on the tail of $\langle f_e \rangle$, where there are few particles. Hence plasma waves are unlikely to influence relaxation in a significant way. On the other hand, ion acoustic waves are resonant in the *bulk* of the electron distribution. Moreover, if $T_e \gg T_i$, it is easy to identify a band of electron velocities with significant population levels f but for which ion Landau damping is negligible. Waves resonant there will be weakly damped, and so may substantially enhance relaxation of $\langle f_e(v) \rangle$. It is this phenomenon of collectively enhanced relaxation that we seek to explore quantitatively.

To explore collective enhancement of relaxation, we process from Eq.(2.47), make a pole expansion around the ion acoustic wave resonance and note for ion acoustic wave, $\omega < \boldsymbol{k} \cdot \boldsymbol{v}$ (for electrons), so

$$B_{\alpha,\beta} = 2\pi q^4 \int_{-\infty}^{\infty} \mathrm{d}\omega \int \mathrm{d}^3k\, \delta(\boldsymbol{k}\cdot\boldsymbol{v})\delta(\boldsymbol{k}\cdot\boldsymbol{v}')\frac{\delta\epsilon_r(\boldsymbol{k},\omega_k)}{|\mathrm{Im}\,\epsilon(\boldsymbol{k},\omega)|}. \tag{2.48}$$

Here $\epsilon_r(\boldsymbol{k}, \omega_k)=0$ for wave resonance, and $e=e'=q$, as scattered and field particles are all electrons. The term $\mathrm{Im}\,\epsilon(\mathbf{k}, \omega)$ refers to the collective mode dissipation rate. Now, changing variables according to

$$\begin{aligned} R &= \boldsymbol{k}\cdot\hat{n}, \\ k_1 &= \boldsymbol{k}\cdot\boldsymbol{v}, \quad k_2 = \boldsymbol{k}\cdot\boldsymbol{v}' \\ \hat{n} &= \boldsymbol{v}\times\boldsymbol{v}'/|\boldsymbol{v}\times\boldsymbol{v}'|. \end{aligned}$$

We have

$$\mathrm{d}^3k = \mathrm{d}R\mathrm{d}k_1\mathrm{d}k_2/|\boldsymbol{v}\times\boldsymbol{v}'|,$$

so the k_1, k_2 integrals in Eq.(2.48) may be immediately performed, leaving

$$B_{\alpha,\beta} = \frac{2\pi q^4 n_\alpha n_\beta}{|\boldsymbol{v}\times\boldsymbol{v}'|}\, 2\int_{R>0}\mathrm{d}k \int_{-\infty}^{\infty}\mathrm{d}\omega\, \frac{\delta(\epsilon_r(\boldsymbol{k},\omega))}{R^2|\mathrm{Im}\,\epsilon|}. \tag{2.49}$$

We remind the reader that this is the piece of $B_{\alpha,\beta}$ associated with field particle speeds or fluctuation phase speeds $v' \sim \omega/k \ll v_{Te}$ for which the collective enhancement is negligible and *total* $J(v)$ is, of course, the *sum* of both these contributions. Now, the dielectric function for ion acoustic waves is,

$$\mathrm{Re}\,\epsilon(k,\omega) = 1 - \frac{\omega_{pi}^2}{\omega^2} + \frac{1}{k^2\lambda_D^2}. \tag{2.50a}$$

$$\mathrm{Im}\,\epsilon(k,\omega) = \sqrt{\frac{\pi}{2}}\frac{\omega}{k^3}\left(\frac{1}{\lambda_{De}^2 v_{Te}} + \frac{1}{\lambda_{Di}^2 v_{Ti}}\mathrm{e}^{-\omega^2/2k^2v_{Ti}^2}\right). \tag{2.50b}$$

Here λ_{De} and λ_{Di} are the electron and ion Debye lengths, respectively. Anticipating the result that

$$\omega^2 = \frac{k^2 c_s^2}{1 + k^2 \lambda_{De}^2}$$

for ion acoustic waves, Eqs.(2.50a, 2.50b) together suggest that the strongest collective enhancement will come from short wavelength (i.e. $k^2\lambda_{De}^2 \gtrsim 1$), because $\mathrm{Im}\,\epsilon(k, \omega)$ is smaller for these scales, since

$$\mathrm{Im}\,\epsilon(k, \omega) \sim \frac{1}{k^2\lambda_{De}^2}\frac{\omega}{k v_{Te}}.$$

For such short wavelengths, then

$$\begin{aligned}\delta(\epsilon_r) &\cong \delta\left(1 - \omega_{pi}^2/\omega^2\right) \\ &= \frac{1}{2}\omega_{pi}\left[\delta(\omega - \omega_{pi}) + \delta(\omega + \omega_{pi})\right].\end{aligned}$$

Evaluating $B_{\alpha,\beta}$, as given by Eqs.(2.48) and (2.49), in this limit then finally gives,

$$\begin{aligned}B_{\alpha,\beta} &= \left(\frac{4\pi q^2 \omega_{pi} n_\alpha n_\beta}{|v \times v'|}\right)\int \frac{\mathrm{d}k}{k^2 |\mathrm{Im}\,\epsilon(k, \omega_{pi})|} \\ &= \frac{2\sqrt{2\pi} q^4 v_{Te} \lambda_{De}^2}{|v \times v'|\lambda_{Di}^2} n_\alpha n_\beta \int \mathrm{d}\xi \left[1 + \exp\left(-\frac{1}{2\xi} + \frac{L}{2}\right)\right]^{-1}, \qquad (2.51a)\end{aligned}$$

where:

$$L = \ln\left[\left(\frac{T_e}{T_i}\right)^2 \frac{m_i}{m_e}\right] \qquad (2.51b)$$

and $\xi = k^2\lambda_{De}^2$. Equation (2.51a) quite clearly illustrates that maximal relaxation occurs for *minimal* $\mathrm{Im}\,\epsilon(\xi, L)$, that is when $\exp[-1/2\xi + L/2] \ll 1$. That is, the collective enhancement of discreteness-induced scattering is determined by $\mathrm{Im}\,\epsilon$ for the least damped mode. This occurs when $\xi \lesssim 1/L$, so that the dominant contribution to $B_{\alpha,\beta}$ comes from scales for which

$$k^2 = (\boldsymbol{k} \cdot \hat{n})^2 < 1/\left(\lambda_{De}^2 L\right).$$

Note that depending on the values of L and the Coulomb logarithm ($\ln \Lambda$, which appears in the standard Coulombic scattering contribution to $B_{\alpha,\beta}$ from $v' \sim v_{Te}$), the collectively enhanced $B_{\alpha,\beta}$ due to low velocity field particles ($v' \ll v_{Te}$) may

even exceed its familiar counterpart Coulomb scattering. Clearly, this is possible only when $T_e/T_i \gg 1$, yet not so large as to violate the tenets of the TPM and B–L theories.

2.2.4 *Test particle model: looking back and looking ahead*

In this section of the introductory chapter, we have presented the test particle model for fluctuations and transport near thermal equilibrium. As we mentioned at the beginning of the chapter, the TPM is the most basic and most successful fluctuation theory for weakly collisional plasmas. So, despite its limitation to stable, quiescent plasmas, the TPM has served as a basic paradigm for treatments of the far more difficult problems of *non-equilibrium* plasma kinetics, such as plasma turbulence, turbulent transport, self-organization etc. Given this state of affairs, we deem it instructive to review the essential elements of the TPM and place the subsequent chapters of this book in the context of the TPM and its elements. In this way, we hope to provide the reader with a framework from which to approach the complex and sometimes bewildering subject of the physical kinetics of non-equilibrium plasmas. The discussion that follows is summarized in Table 2.3. We discuss and compare the test particle model to its non-equilibrium descendents in terms of both physics concepts and theoretical constructs.

Regarding *physics concepts*, the TPM is fundamentally a "near-equilibrium" theory, which presumes a balance of emission and absorption at each k. In a turbulent plasma, non-linear interaction produces spectral transfer and a spectral cascade, which de-localize the location of absorption from the region of emission in k, ω space. A spectral transfer turbulence energy from one region (i.e. emission) to another (i.e. damping). There two cases are contrasted in Figure 2.1.

A second key concept in the TPM is that emission occurs *only* via Cerenkov radiation from discrete test particles. Thus, since the only source for collective modes is discreteness, we always have

$$\nabla \cdot \epsilon E = 4\pi q \delta(x - x(t)),$$

so

$$\left\langle \phi^2 \right\rangle_{\mathbf{k},\omega} = \frac{\langle \tilde{n}^2 \rangle}{|\epsilon(\mathbf{k}, \omega)|^2}.$$

In contrast, for non-equilibrium plasmas, nonlinear coupling produces incoherent emission so the energy in mode k evolves according to,

Table 2.3. *Test particle model and its non-equilibrium descendents: physical concepts and theoretical constructs*

Test particle model	Non-equilibrium descendent
Physics concepts	
Emission versus absorption balance per $\boldsymbol{k}$	Spectral cascade, transfer, inertial range (Chapter 5, 6)
Discreteness noise	Incoherent mode-coupling (Chapter 5, 6), granulation emission (Chapter 8)
Relaxation by screened collisions	Collective instability-driven relaxation, quasi-linear theory, granulation interaction (Chapter 3, 8)
Theoretical constructs	
Linear response unperturbed orbit	Turbulence response, turbulent diffusion, resonance broadening (Chapter 4, 6)
Damped mode response	Nonlinear dielectric, wave–wave interaction, wave kinetics (Chapter 5, 6)
Mean-field theory	Mean-field theory without and with granulations (Chapter 3, 8)
Discreteness-driven stationary spectrum	Wave kinetics, renormalized mode coupling, disparate scale interaction (Chapter 5 – 7)
Balescu–Lenard, screened Landau equations	Quasi-linear theory, Granulation relaxation theory (Chapter 3, 8)

$$\frac{\partial}{\partial t}\left\langle E^2\right\rangle_k + \left(\sum_{k'} C(\boldsymbol{k},\boldsymbol{k}')\left\langle E^2\right\rangle_{k'} \mathcal{T}_{c_{k,k'}}\right)\left\langle E^2\right\rangle_k + \gamma_{dk}\left\langle E^2\right\rangle_k$$
$$= \sum_{\substack{p,q \\ p+q=k}} C(\boldsymbol{p},\boldsymbol{q})\tau_{c\ p,q}\left\langle E^2\right\rangle_p \left\langle E^2\right\rangle_q + S_{Dk}\left\langle E^2\right\rangle_k, \tag{2.52}$$

where S_{Dk} is the discreteness source and γ_{dk} is the linear damping for the mode $\boldsymbol{k}$ (Kadomtsev, 1965). For sufficient fluctuation levels, the nonlinear noise term (i.e. the first on the right-hand side) will clearly dominate over discreteness. A similar comment can be made in the context of the left-hand side of Eq.(2.52), written above. Nonlinear damping will similarly eclipse linear response damping for sufficiently large fluctuation levels.

A third physics concept is concerned with the mechanism ~~physics~~ of relaxation and transport. In the TPM, these occur only via screened collisions. Collective effects associated with weakly damped modes may enhance relaxation but do not fundamentally change this picture. In a non-equilibrium plasma, collective modes

can drive relaxation of the unstable $\langle f \rangle$, and nonlinear transfer can couple the relaxation process, thus enhancing its rate.

In the realm of *theoretical constructs* and methods, *both* the test particle model and its non-equilibrium counterparts are fundamentally mean-field type approaches. However, they differ dramatically with respect to particle and model responses, nature of the wave spectrum and in how relaxation is calculated. The TPM assumes linear response theory is valid, so particle response functions exhibit only 'bare' Landau resonances. In contrast, scattering by strong electric field fluctuations will *broaden* the Landau resonance and *renormalize* the Landau propagator, so that,

$$R_{k,\omega} \sim \mathrm{e}^{ikx} \int_0^\infty \mathrm{e}^{i\omega\tau} \mathrm{e}^{-ikx(-\tau)} \mathrm{d}\tau$$
$$\sim \int_0^\infty \mathrm{e}^{i(\omega - kv)\tau} \mathrm{d}\tau = i/(\omega - kv) \tag{2.53a}$$

becomes,

$$R_{k,\omega} \sim \int_0^\infty \mathrm{e}^{i\omega\tau}\, \mathrm{e}^{-ikx_0(-\tau)} \left\langle \mathrm{e}^{-ik\delta x(-\tau)} \right\rangle \mathrm{d}\tau$$
$$\sim \int_0^\infty \mathrm{e}^{i(\omega - kv)\tau - \frac{k^2 D}{3}\tau^3} \mathrm{d}\tau \sim i/(\omega - kv + i/\tau_c), \tag{2.53b}$$

where $1/\tau_c = (k^2 D/3)^{1/3}$. This is equivalent to the renormalization

$$\left[-i(\omega - kv) \right]^{-1} \to \left[-i(\omega - kv) - \frac{\partial}{\partial v} D \frac{\partial}{\partial v} \right]^{-1}. \tag{2.53c}$$

Here $D = D[\langle E^2 \rangle]$ is a functional of the turbulence spectrum. In a similar way to that sketched in Eq.(2.53), collective responses are renormalized and broadened by nonlinear wave interaction. Moreover, in the non-equilibrium case, a separate wave kinetic equation for $N(k, \boldsymbol{x}, t)$, the wave population density, is required to evolve the wave population in the presence of sources, non-linear interaction and refraction, etc. by disparate scales. This wave kinetic equation is usually written in the form,

$$\frac{\partial N}{\partial t} + (\boldsymbol{v}_\mathrm{g} + \boldsymbol{v}) \cdot \nabla N - \frac{\partial}{\partial \boldsymbol{x}}(\omega + \boldsymbol{k} \cdot \boldsymbol{v}) \cdot \frac{\partial N}{\partial \boldsymbol{k}} = S_k N + C_K(N). \tag{2.54}$$

Since in practical problems, the mean field or coarse grained wave population density $\langle N \rangle$ is of primary interest, a similar arsenal of quasi-linear type closure techniques has been developed for the purpose of extracting $\langle N \rangle$ from the wave